Pownall, H. J., & Smith, L. C. (1973) *J. Am. Chem. Soc. 95*, 3136-3140.
Rintoul, D. A., Chou, S. M., & Silbert, D. F. (1979) *J. Biol. Chem. 254*, 10070-10077.
Rose, J. K., & Gallione, C. J. (1981) *J. Virol. 39*, 519-528.
Roseman, M. A., & Thompson, T. E. (1980) *Biochemistry 19*, 439-444.
Schloemer, R. H., & Wagner, R. R. (1975) *J. Virol. 16*, 237-249.
Selinger, Z., & Lapidot, Y. (1966) *J. Lipid Res. 7*, 174-175.
Silvus, J. R. (1982) in *Lipid-Protein Interactions* (Jost, P., & Griffith, O. M., Eds.) Vol. 2, p 239, Wiley, New York.
Verkleij, A. J., DeKruijff, B., Ververgaert, P. H., Tocanne, J. F., & Van Deenen, L. L. M. (1974) *Biochim. Biophys. Acta 339*, 432-437.
Wagner, R. R. (1975) *Comp. Virol. 4*, 1-93.
Wiener, J. R., Pal, R., Barenholz, Y., & Wagner, R. R. (1983a) *Biochemistry 22*, 2162-2170.
Wiener, J. R., Wagner, R. R., & Freire, E. (1983b) *Biochemistry 22*, 6117-6123.
Zakowski, J. J., & Wagner, R. R. (1980) *J. Virol. 36*, 93-102.
Zakowski, J. J., Petri, W. A., Jr., & Wagner, R. R. (1981) *Biochemistry 20*, 3902-3907.

Hydrogen Exchange of Individual Amide Protons in the F Helix of Cyanometmyoglobin†

N. Vasant Kumar and N. R. Kallenbach*
Department of Biology, University of Pennsylvania, Philadelphia, Pennsylvania 19104
Received May 3, 1985

ABSTRACT: Hydrogen exchange of the individual amide protons of alanine-90 (F5), glutamine-91 (F6), serine-92 (F7), and histidine-93 (F8) residues in cyanometmyoglobin of sperm whale has been studied by ^{1}H nuclear magnetic resonance spectroscopy at 360 MHz. The amide proton resonances of F5, F6, and F7 have been assigned by use of the selective nuclear Overhauser effect between the consecutive amide protons. At pH 6.8, and in the temperature range of 5-20 °C, these protons show a 10^4-fold retardation compared to the rates in free peptides. Apparent activation enthalpies for hydrogen exchange of F5, F6, and F8 protons are 18.5 ± 0.4, 9.5 ± 0.3, and 18.5 ± 0.3 kcal/mol, respectively. Some implications of these results on the nature of the opening processes involved in hydrogen exchange are considered.

Hydrogen exchange (HX)[1] of peptide NH protons with solvent protons (Hvidt & Nielsen, 1966; Woodward & Hilton, 1979; Englander & Kallenbach, 1984) has provided a powerful technique to investigate protein folding (Brems & Baldwin, 1984; Kuwajima et al., 1984), dynamics (Hilton & Woodward, 1978; Wagner & Wuthrich, 1979a; Wuthrich & Wagner, 1979), and also functional labeling or allosteric effects (Englander & Englander, 1983; Englander et al., 1983). Linderstrom-Lang first attempted to correlate hydrogen exchange behavior with protein dynamics at a time when little was known about the three-dimensional structure of proteins (Linderstrom-Lang & Schellman, 1959). The detailed mechanism of amide proton exchange in proteins still remains elusive and has been a controversial subject in contemporary biophysical chemistry (Englander & Kallenbach, 1984). Two extreme models—local unfolding (or breathing) and solvent penetration—have been proposed to account for the observed HX behavior of proteins. In the local unfolding model, the protein is assumed to undergo a transient cooperative structural unfolding with the exchange event occurring in a medium much like the bulk solvent. In solvent penetration models, on the other hand, the exchange is limited by the accessibility of each individual site to the solvent. In this case, the exchange may take place in the interior of the protein. A detailed understanding of the mechanism is essential to exploit the potential of the HX technique to probe protein structure, dynamics, and function.

In the present study, we report the HX behavior of four consecutive amide protons within the F helix of myoglobin as measured by NMR spectroscopy directly. Application of NMR spectroscopy for measuring exchange offers the advantage over other solution techniques that the rates can be measured for individual amide proton sites (Hilton & Woodward, 1978; Richarz et al., 1979; Wagner et al., 1984). Assignment of the resonances is a prerequisite for this approach to succeed. In general, the problem of NMR spectral assignments becomes increasingly difficult as the molecular size increases. Large numbers of signals, limited dispersion in chemical shifts, and relatively broad signals due to slow tumbling of macromolecules all result in loss of resolution. Assignment of the exchangeable protons in H_2O is further complicated by the dynamic range problem due to the very intense solvent peak (Redfield et al., 1975). The fact that only one amide NH proton (His F8) in sperm whale myoglobin (153 residues) has been assigned so far reflects some of these difficulties. In the present study, we have assigned three more consecutive amide protons on the basis of NH-NH-type NOEs. The hydrogen exchange behavior of consecutive protons in the F helix provides useful clues about protein flexibility as well as the fundamental mechanism of HX in these secondary structures. Myoglobin has been chosen as a model system for two reasons. First, dynamics are intrinsically relevant to function in this protein since there is no static channel available in the molecule for oxygen to reach the heme group (Case & Karplus, 1979). Second, its structure in deoxy

†Supported by National Institutes of Health Grant GM 31861.

[1] Abbreviations: NMR, nuclear magnetic resonance; NOE, nuclear Overhauser effect; MbCN, cyanometmyoglobin; HX, hydrogen exchange; His, histidine; Ser, serine; Gln, glutamine; Pro, proline; FID, free induction decay.

0006-2960/85/0424-7658$01.50/0

and oxy forms is well-known to high resolution (Takano, 1977a,b; Phillips, 1980). The F helix (residues 86–94 in sperm whale myoglobin) forms part of the lining of the heme pocket by enclosing part of the proximal side of the heme group. His F8 is liganded to iron of the heme moiety (Takano, 1977a,b; Dickerson & Geis, 1983). Moreover, the X-ray crystal structure of oxymyoglobin shows significant displacement in the region of the F helix upon oxygen binding to myoglobin (Phillips, 1980).

Experimental Procedures

Sperm whale myoglobin was purchased from Sigma and used without further purification. In all the experiments, 70 mg of the protein was dissolved in 0.4 mL of solvent containing 100 mM KCl and a 9-fold excess of KCN. Undissolved material, if any, was removed by centrifugation. The pH was measured by using the glass electrode and corrected for the isotope effects in D_2O. The NMR experiments were carried out on a 360-MHz modified Bruker spectrometer. Spectra in 90% H_2O were obtained by using a time-shared Redfield pulse sequence (Redfield & Kunz, 1979) with the radio-frequency (rf) carrier located approximately 5 kHz downfield from the water signal. Spectra in D_2O were obtained by saturating the residual water resonance at all times except during acquisition of the FID. Difference NOE experiments were performed by using the following pulse sequence: $\{[-\tau(\omega_{off})$–rf pulse–RD–$]_{32}$ minus $[-\tau(\omega_{on})$–rf pulse–RD–$]_{32}\}_{128}$ where ω_{on} is the resonance frequency of interest, ω_{off} is an off-resonance frequency, τ is the presaturation time (0.25 s), the rf pulse is the time-shared Redfield pulse sequence, and RD is the relaxation delay. As indicated, on-resonance and off-resonance experiments in groups of 32 scans were performed alternately, and the subtraction was carried out directly on the FIDs prior to Fourier transformation. Kinetics of hydrogen exchange were studied by dissolving the protein in D_2O buffer and measuring the signal height in the ^1H NMR spectrum as a function of time. In each case, 1024 scans were accumulated at uniform time intervals over a period of 10 min. The midpoint of the time duration is taken as the corresponding time of exchange. The intensity of each signal was observed to decrease exponentially with time, i.e., $I(t) = I(0)\exp(-kt)$, where k is the rate constant, t is time, and I the intensity. The exchange rates were obtained from least-squares analysis of the semi-log plots of signal heights as a function of time. Activation enthalpies were calculated from the Arrhenius plots of the exchange rates.

Results and Discussion

Assignments. As a first step toward assignment of the amide protons of the F helix, we have identified resonances from the exchangeable protons by comparing the low-field region of ^1H NMR spectra of cyanometmyoglobin (MbCN) in H_2O and D_2O (Figure 1) at pH 6.8. The absence of signals labeled a–g in the D_2O spectrum clearly shows that these resonances correspond to exchangeable protons in MbCN. In addition to these resolved peaks, there are several other resonances in the spectral region of 6–8 ppm. The resonances a and b were previously assigned to the peptide NH of His F8 and to N_1H of the His FG1 side chain (Sheard et al., 1970; Cutnell et al., 1981).

We have used the selective nuclear Overhauser effect (NOE) to assign the other exchangeable protons. From the crystal structure, it is known that residues Leu[86]-Lys-Pro-Leu-Ala-Gln-Ser-His-Ala[94], labeled F1, F2, ..., F9, form an α-helix which is interrupted by Pro F3 (Takano, 1977a,b; Dickerson & Geis, 1983). Consecutive amide protons (i and

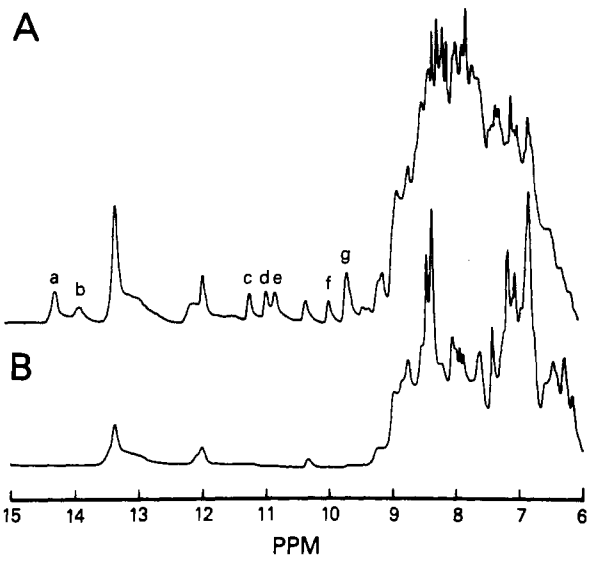

FIGURE 1: Part of the 360-MHz ^1H NMR spectra of cyanometmyoglobin in H_2O (A) and in D_2O (B) at pH 6.8 and 10 °C. The resonances labeled a–g correspond to exchangeable protons. The signal a has been assigned to the amide proton of the His F8 residue.

$i \pm 1$) in an α-helix are separated by approximately 2.8 Å (Wuthrich et al., 1984). Dipolar interaction which is proportional to r_{ij}^{-6}, where r_{ij} is the distance between nuclei i and j, is very effective at these short distances (Noggle & Shirmer, 1971). Such cross-relaxation processes should result in an observable NOE between the consecutive amide protons in an α-helix (Wuthrich et al., 1984) whenever the helix is not very flexible. Results from a set of NOE experiments on MbCN are shown in Figure 2. When resonance a corresponding to the amide proton of His F8 is saturated, prominent NOEs are observed to the exchangeable peak c at 11.2 ppm as well as to the nonexchangeable peaks at 13.3, 12.1, and 10.3 ppm (Figure 2B). Assignment of peak c is crucial for the subsequent assignments. Let us consider the possible candidates which might be assigned to peak c. Neutron diffraction data on (carbonmonoxy)myoglobin which is a good model for MbCN show that the amide protons of F7 and F9, the side chain N_1H proton of His F8, and the OH proton of Ser F7 are separated from the amide proton of His F8 by distances of 2.64, 2.59, 2.52, and 3.47 Å, respectively (Hanson & Schoenborn, 1981). In principle, saturation of the amide proton of His F8 can show an NOE to each of these protons. However, the N_1H of His F8 has been previously assigned to a peak at 22 ppm (Sheard et al., 1970; Cutnell et al., 1981). We do observe an NOE at this frequency when peak a is saturated (not shown in Figure 2). The neutron diffraction data show that the OH proton of Ser F7 is also close (2.55 Å) to the N_1H proton of His F8. If peak c corresponds to the OH proton of Ser F7, we expect to observe an NOE at the resonance frequency of the His N_1H on saturating peak c. However, saturation of peak c does not show any NOE to the N_1H of His F8, suggesting that peak c does not correspond to the OH of Ser F7. We are left with a choice between the amide protons of Ser F7 and Ala F9. Distance considerations alone cannot discriminate between these two alternatives. Crystallographic results show that the region including the C-terminus of the F-helix and the FG corner is highly dynamic and relatively easily accessible to the solvent (Frauenfelder & Petsko, 1980; Hartmann et al., 1982). It is thus reasonable to assume that the flexibility of the helix in this region makes the NOE between F8 and F9 amide protons very weak and unobservable. For these reasons, peak c is assigned to the

Table I: Exchange Rates of Amide Protons of the F Helix

	$k_{ex} \times 10^3$ (min^{-1})[a] at temp (°C)				k_{calcd}[b] (min^{-1})	R[c] $\times 10^{-4}$ at 10 °C
	5	10	15	20		
F5	0.5 ± 0.02	1.2 ± 0.1	2.1 ± 0.2	3.1 ± 0.1	69.8	5.8
F6	2.7 ± 0.1	3.4 ± 0.1	5.2 ± 0.3	6.4 ± 0.3	97.7	2.9
F7		fast			310.5	
F8	2.2 ± 0.1	4.6 ± 0.1	8.5 ± 0.2	12.0 ± 0.5	218.8	4.8

[a] Measured rate constants. [b] Calculated rate constants at pH 6.8 and 10 °C according to the equation suggested by Englander & Englander (1978). [c] Retardation factors, k_{calcd}/k_{ex}.

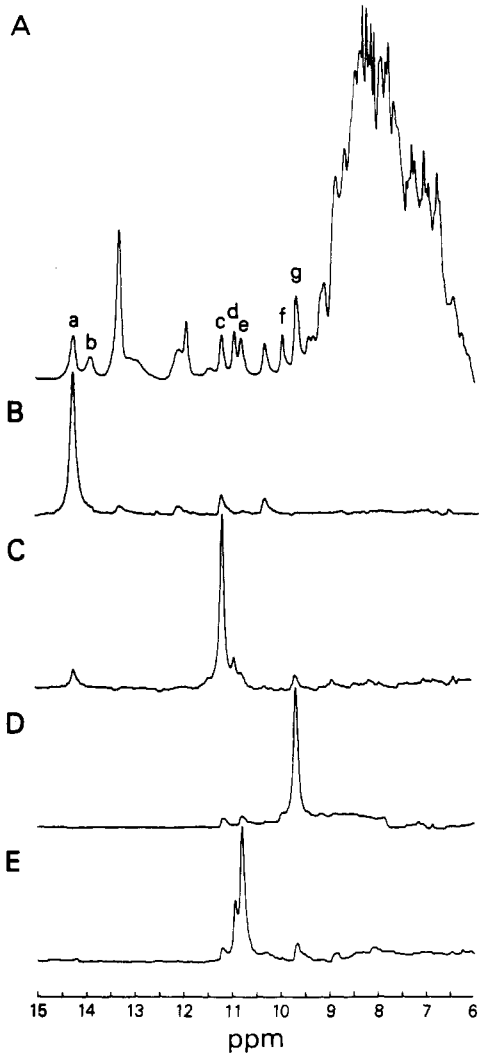

FIGURE 2: Results of selective NOE experiments on cyanometmyoglobin in H_2O at pH 6.8 and 10 °C. The presaturation time is 0.25 s in these experiments, and all the NOEs in this figure are actually negative. (A) Normal spectrum in H_2O at pH 6.8 and 10 °C. The resonances corresponding to the exchangeable protons are labeled a–g. Peak a has been assigned to the amide proton of the His F8 residue. (B) Difference NOE spectrum resulting from the saturation of peak a (F8 amide proton). Peak c is assigned to the amide proton of Ser F7. (C) Difference NOE spectrum corresponding to the presaturation of peak c. (D) Peak g is saturated in this experiment. (E) Difference NOE spectrum when peak e is saturated.

amide proton of Ser F7. Further assignments are then relatively straightforward. Saturation of peak c shows an NOE to the His F8 amide proton (peak a), as expected, and another one to peak g (9.68 ppm). Since peak g should be from an amide proton of the adjacent residue to Ser F7, and peak a is assigned to the amide proton of His F8, resonance g should correspond to the amide proton of Gln F6. The signal e (10.82 ppm) is assigned to the amide proton of Ala F5 since an NOE at this frequency is observed on saturating the amide proton

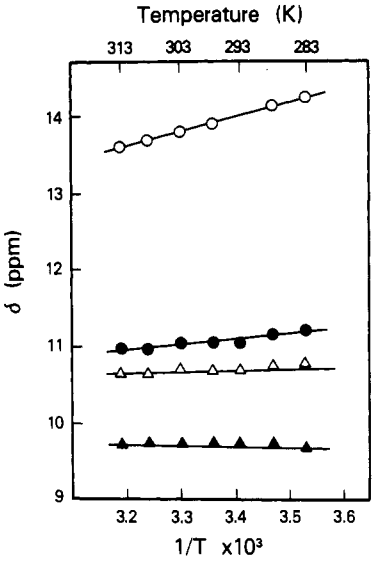

FIGURE 3: Effect of temperature on the chemical shifts (δ) of the amide protons of F5 (△), F6 (▲), F7 (●), and F8 (○). Chemical shifts are plotted as a function of $1/T$. Corresponding temperatures (in degrees kelvin) are shown on the top.

of F6 (peak g) (Figure 2D,E). No NOE to a new peak is observed when amide NH of F5 is saturated. It is possible that the presence of a proline residue at the F3 position distorts the helix in this region.

Variation of chemical shifts (δ) of the amide protons of F5, F6, F7, and F8 as a function of inverse temperature (T^{-1}) is shown in Figure 3. All four amide protons show a linear dependence with T^{-1}, consistent with the idea that the pseudocontact interaction with iron is primarily responsible for the observed shifts. Contribution from the contact shifts which also show a linear dependence of T^{-1} is expected to be negligible, if any, since these protons are separated from iron by several covalent bonds. The proximity of the F8 amide proton to iron is reflected in the significant variation of its chemical shift with temperature. In fact, the magnitude of chemical shifts and their variation with temperature are consistent with the corresponding distances from the iron atom of the heme group.

Hydrogen Exchange Behavior of the F Helix. We have studied the hydrogen exchange rates of the individual amide protons F5–F8 at pH 6.8 over the temperature range 5–20 °C. The amide proton of Ser F7 exchanges too rapidly to be measured by the direct methods used here, even at 0 °C. Representative data at 10 and 20 °C are shown in Figures 4 and 5, respectively. These data show that the exchange of F5, F6, and F8 protons obeys pseudo-first-order kinetics; i.e., the signal intensity decreases exponentially with time. HX rates of these protons at various temperatures are summarized in Table I. In general, the rates are in the order F7 ≫ F8 > F6 > F5. Expected rates at pH 6.8 and 10 °C for the random-coil as calculated from Molday factors (Molday et al., 1972; Englander & Englander, 1978) are 69.8, 97.7, 310.5,

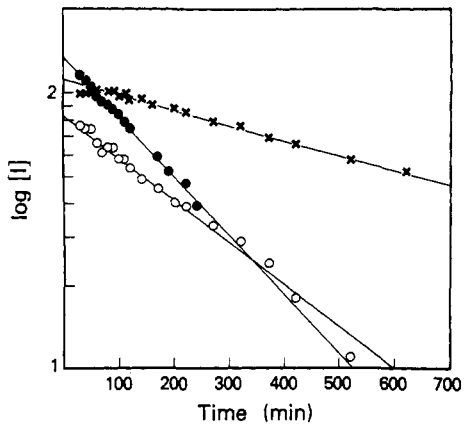

FIGURE 4: Hydrogen exchange kinetics of F5 (×), F6 (○), and F8 (●) amide protons at pH 6.8 and 10 °C. I is the peak intensity and t the time in minutes in this semi-log plot.

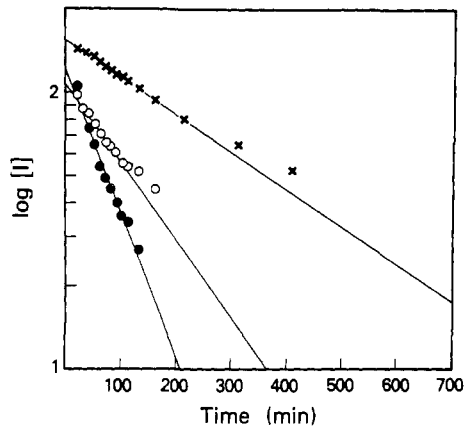

FIGURE 5: Kinetics of hydrogen exchange of F5 (×), F6 (○), and F8 (●) amide protons at pH 6.8 and 20 °C. I is the peak intensity and t the time in minutes in this semi-log plot.

and 218.8 min^{-1} for F5, F6, F7, and F8, respectively. The measured rates under these conditions show that there is a 10^4-fold retardation in exchange for these protons. It is interesting that the observed rates in the folded structure of myoglobin follow the same relative trends as in the random-coil.

Variation of the HX rates as a function of temperature is shown in Figure 6. These results show that the Arrhenius equation is valid in the temperature range of 5–20 °C. Apparent activation enthalpies are 18.5 ± 0.4, 9.5 ± 0.3, and 18.5 ± 0.3 kcal/mol for F5, F6, and F8 amide protons, respectively. It is surprising that the activation enthalpy of F6 is significantly lower and different from that of F5 and F8. Implications of this behavior in terms of the HX mechanism are discussed below.

The crystal structure of myoglobin shows that the axis of the F helix is oriented almost parallel to the average heme plane. Of the four amide protons we are concerned with, the F8 amide proton is most shielded from the solvent. The amide protons F5 and F6, by comparison, lie on the surface and should have easy accessibility to the solvent. A simple penetration model would predict that the F8 amide proton, of the four protons, exchanges most slowly. Experimental rates in fact show that the exchange rate of F8 is higher than that of F5 or F6 amide protons. Even if the inductive effects of the nearest neighbors (i.e., Molday effects) are operative in the folded conformation as well, the observed activation enthalpies are not easily explained by a penetration model. The amide protons F5, F6, and F8 have retardation factors of approxi-

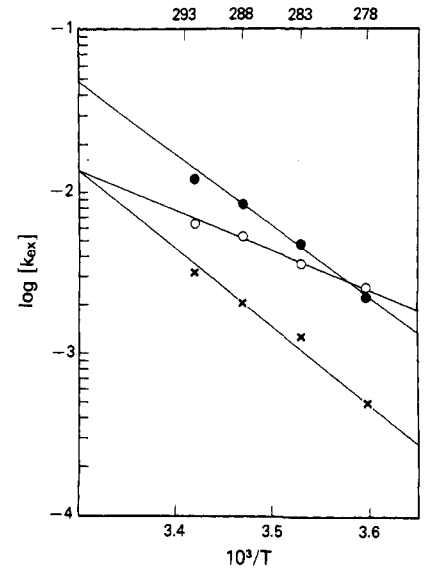

FIGURE 6: Arrhenius plot of the exchange rates (k_{ex}) of F5 (×), F6 (○), and F8 (●) amide protons in cyanometmyoglobin at pH 6.8. log k_{ex} is plotted as a function of $1/T$. Corresponding temperatures (in degrees kelvin) are shown on the top.

mately 6×10^4, 3×10^4, and 5×10^4, respectively (Table I). Similarity in these retardation factors suggests that a "local unfolding" model can describe their exchange. For example, opening of at least one turn of the helix could expose each of these amide protons to the solvent. However, the activation enthalpy for the exchange of the F6 amide proton is 9.5 kcal/mol which is significantly lower than the enthalpies for F5 and F8 amide protons. Further, F7 exchanges more rapidly than the other three protons. Could the structural fluctuations, responsible for transient opening of hydrogen bonds in the α-helix, be distinct for different sites within a helix? For instance, Wagner et al. (1984) suggested that three different fluctuations might be involved in the opening of the C-terminal helix of bovine pancreatic trypsin inhibitor and its analogues. Though this model is simple, it poses some difficulties regarding the cooperative nature of the helices. Results on the helix–coil transitions in synthetic model α-helices suggest that individual bonds in an α-helix are not independent but interact strongly with the next neighbor units (Scheraga, 1978). Short helical units in globular proteins are still more cooperative (Creighton, 1984). Data for comparable helices in apamin and RNase S peptide show a roughly uniform retardation pattern in the exchange rates of peptides not adjacent or close to the ends (Englander & Kallenbach, 1984; Kuwajima et al., 1983). In fact, strong "end effects" in the HX rates of individual amides that initiate or terminate short α-helices can be taken to indicate that the open states may be cooperative. If this is so, despite the clear difference between denaturation of the helix and transient opening of the helix to allow exchange, both processes should involve coupling of neighboring residues. If, on the other hand, the end effect of hydrogen exchange is attributed to dynamic processes in which local internal motions are more damped than near the ends, a localized opening reaction could be possible. We believe that more comparative examples are required to settle this issue.

Registry No. H_2, 1333-74-0.

REFERENCES

Brems, D. N., & Baldwin, R. L. (1984) *J. Mol. Biol. 180*, 1141–1156.

Case, D. A., & Karplus, M. (1979) *J. Mol. Biol. 132*, 343–368.

Creighton, T. E. (1984) in *Proteins: Structure and Molecular Properties*, pp 265-333, W. H. Freeman, New York.
Cutnell, J. D., La Mar, G. N., & Kong, S. B. (1981) *J. Am. Chem. Soc. 103*, 3567-3572.
Dickerson, R. E., & Geis, I. (1983) in *Hemoglobin: Structure, Function, Evolution and Pathology*, pp 26-33, Benjamin/Cummings, Menlo Park, CA.
Englander, J. J., Rogero, J. R., & Englander, S. W. (1983) *J. Mol. Biol. 169*, 325-344.
Englander, S. W., & Poulsen, A. (1969) *Biopolymers 7*, 379-393.
Englander, S. W., & Englander, J. J. (1978) *Methods Enzymol. 49*, 24-39.
Englander, S. W., & Englander, J. J. (1983) in *Structure and Dynamics: Nucleic Acids and Proteins* (Clementi, E., & Sarma, R. H., Eds.) pp 421-433, Adenine Press, New York.
Englander, S. W., & Kallenbach, N. R. (1984) *Q. Rev. Biophys. 16*, 521-655.
Frauenfelder, H., & Petsko, G. A. (1980) *Biophys. J. 32*, 465-483.
Hanson, J., & Schoenborn, B. (1981) *J. Mol. Biol. 153*, 117-146.
Hartmann, H., Parak, F., Steigmann, W., Petsko, G. A., Ponzi, D. R., & Frauenfelder, H. (1982) *Proc. Natl. Acad. Sci. U.S.A. 79*, 4967-4971.
Hilton, B. D., & Woodward, C. K. (1978) *Biochemistry 17*, 3325-3332.
Hvidt, A., & Nielsen, S. O. (1966) *Adv. Protein Chem. 21*, 287-386.
Kuwajima, K., & Baldwin, R. L. (1983) *J. Mol. Biol. 169*, 299-323.
Kuwajima, K., Kim, P. S., & Baldwin, R. L. (1984) *Biopolymers 22*, 59-67.
Linderstrom-Lang, K. U., & Schellman, J. A. (1959) *Enzymes, 2nd Ed. 1*, 443-510.
Molday, R. S., Englander, S. W., & Kallen, R. G. (1972) *Biochemistry 11*, 150-158.
Noggle, J. H., & Shirmer, R. E. (1971) *The Nuclear Overhauser Effect*, Academic Press, New York.
Phillips, S. E. V. (1980) *J. Mol. Biol. 142*, 531-554.
Redfield, A. G., & Kunz, S. D. (1979) in *NMR and Biochemistry* (Opella, S. J., & Lu, P., Eds.) pp 225-239, Marcel Dekker, New York.
Redfield, A. G., Kunz, S. D., & Ralph, E. K. (1975) *J. Magn. Reson. 19*, 114-117.
Richarz, R., Sehr, P., Wagner, G., & Wuthrich, K. (1979) *J. Mol. Biol. 130*, 19-30.
Scheraga, H. A. (1978) *Pure Appl. Chem. 50*, 315-324.
Sheard, B., Yamane, T., & Shulman, R. G. (1970) *J. Mol. Biol. 53*, 35-48.
Takano, T. J. (1977a) *J. Mol. Biol. 110*, 537-568.
Takano, T. J. (1977b) *J. Mol. Biol. 110*, 569-584.
Wagner, G., & Wuthrich, K. (1979a) *J. Mol. Biol. 130*, 31-37.
Wagner, G., & Wuthrich, K. (1979b) *J. Mol. Biol. 134*, 75-94.
Wagner, G., Stassinopoulou, C. I., & Wuthrich, K. (1984) *Eur. J. Biochem. 145*, 431-436.
Woodward, C. K., & Hilton, B. D. (1979) *Annu. Rev. Biophys. Bioeng. 8*, 99-127.
Wuthrich, K., Billeter, M., & Braun, W. (1984) *J. Mol. Biol. 180*, 715-740.

Equilibrium Denaturation of Pituitary- and Recombinant-Derived Bovine Growth Hormone

David N. Brems,* Scott M. Plaisted, Henry A. Havel, E. Wayne Kauffman, John D. Stodola, Leslie C. Eaton, and Robert D. White

Control Division, The Upjohn Company, Kalamazoo, Michigan 49001

Received May 3, 1985

ABSTRACT: Holladay and co-workers [Holladay, L. A., Hammonds, R. G., & Puett, D. (1974) *Biochemistry 13*, 1653-1661] reported the presence of an equilibrium intermediate in the guanidine hydrochloride (GdnHCl) induced denaturation of pituitary-derived bovine growth hormone (p-bGH). Since then, numerous reports have appeared demonstrating the inherent heterogeneity in p-bGH. In this report we show that a standard preparation of p-bGH can be separated into two components of almost equal abundance differing in molecular weight by approximately 1000. Each of these two components could give rise to different denaturation transitions which would be interpreted as evidence for equilibrium intermediates. We report here the equilibrium denaturation of bGH produced by *Escherichia coli* through recombinant DNA technology. The recombinant-derived bGH (r-bGH) is more homogeneous than that derived from pituitary sources and is greater than 95% a single polypeptide entity. Nevertheless, the GdnHCl-induced denaturation profiles of both recombinant bGH and pituitary bGH are very similar. The presence of equilibrium intermediates is verified by the asymmetry of the denaturation transition as measured by size-exclusion high-performance liquid chromatography and by noncoincidence of the denaturation transitions as observed by ultraviolet absorbance, fluorescence intensity, and circular dichroism. These findings conclusively show that the secondary structure of bovine growth hormone is more stable than the tertiary structure and is consistent with a framework model of protein folding.

A fundamental problem remaining in biology today is that of protein folding; that is, how does a random polypeptide chain fold to a highly ordered conformation? Answers to the protein folding problem would help in determining the code by which the amino acid sequence of a protein specifies its tertiary structure. This would aid in the engineering of changes in protein structure through the use of recombinant DNA techniques. Studies of reversible denaturation reactions of

0006-2960/85/0424-7662$01.50/0